One dimensional acoustic direct nonlinear inversion using the Volterra inverse scattering series

2014 Inverse Problems 30 075006

(http://iopscience.iop.org/0266-5611/30/7/075006)

IOP Publishing Inverse Problems
Inverse Problems **30** (2014) 075006 (17pp) doi:10.1088/0266-5611/30/7/075006

One dimensional acoustic direct nonlinear inversion using the Volterra inverse scattering series

Jie Yao[1], Anne-Cécile Lesage[2,4], Bernhard G Bodmann[3], Fazle Hussain[1,4] and Donald J Kouri[1,2]

[1] Department of Mechanical Engineering, University of Houston, Houston, TX, USA
[2] Department of Physics, University of Houston, Houston, TX, USA
[3] Department of Mathematics, University of Houston, Houston, TX, USA
[4] Department of Mechanical Engineering, Texas Tech University, Lubbock, TX, USA

E-mail: yjie2@uh.edu, alesage@uh.edu, bgbodmann@uh.edu, fazle.hussain@ttu.edu and kouri@central.uh.edu

Received 2 January 2014, revised 7 April 2014
Accepted for publication 6 May 2014
Published 25 June 2014

Abstract

Direct inversion of acoustic scattering problems is nonlinear. One way to treat the inverse scattering problem is based on the reversion of the Born–Neumann series solution of the Lippmann–Schwinger equation. An important issue for this approach is the radius of convergence of the Born–Neumann series for the forward problem. However, this issue can be tackled by employing a renormalization technique to transform the Lippmann–Schwinger equation from a Fredholm to a Volterra integral form. The Born series of a Volterra integral equation converges absolutely and uniformly in the entire complex plane. We present a further study of this new mathematical framework. A Volterra inverse scattering series (VISS) using both reflection and transmission data is derived and tested for several acoustic velocity models. For large velocity contrast, series summation techniques (e.g., Cesàro summation, Euler transform, etc) are employed to improve the rate of convergence of VISS. It is shown that the VISS method with summation techniques can provide a relatively good estimation of the velocity profile. The method is fully data-driven in the respect that no prior information of the model is required. Besides, no internal multiple removal is needed. This one dimensional VISS approach is useful for inverse scattering and serves as an important step for studying more complicated and realistic inversions.

Keywords: inverse scattering series, direct nonlinear inversion, Volterra renormalization, series summation techniques, acoustic scattering

(Some figures may appear in colour only in the online journal)

1. Introduction

Scattering plays a significant role in studying the properties of matter and has enormous applications for both practical and theoretical areas, such as quantum physics, geophysics, medical imaging, nondestructive testing, etc The forward scattering problem involves constructing the scattered field for given targets. The inverse scattering problem determines one or more properties of the target from the measurement of the scattered field. Inverse acoustic scattering has undergone a long study and the methods developed are extensive. The principal state of the art inverse methods can be divided into two categories: (1) the linearized approximation inversion (e.g., Cohen and Bleistein 1977, Bleistein 1984, Clayton and Stolt 1981, Amundsen *et al* 2005) , which usually uses the Born approximation or Rytov approximation of the Lippmann–Schwinger equation to develop a forward equation relating the measured data to the scattering potential. The limitation of the method is that it entails the small-contrast assumption which means the reference and actual medium should be close. (2) model matching methods (e.g., Tarantola 1984, Colton and Monk 1989, Colton and Kress 1998, Pratt 1999, Sirgue and Pratt 2004, Virieux and Operto 2009, Guitton and Alkhalifah 2013), which define a misfit function and try to minimize it to acquire the best-fitting model. One shortcoming of this method is its huge computational cost, which often requires solving the forward problems in an inverse sense. It also requires accurate starting models and regularization techniques.

Based on the early work of Jost and Kohn (1952), Moses (1956), Razavy (1975) and Prosser (1969), Weglein and co-workers developed a general approach, called the inverse scattering series method (Weglein *et al* 1997, 2000, Weglein and F 2001, Weglein *et al* 2003, Shaw 2005, Zhang and Weglein 2009). The method uses the Born–Neumann series solution of the acoustic Lippmann–Schwinger equation and a related expansion of the potential in 'orders of the data'. Each term of the potential is determined in terms of the scattering data and a reference Green's function. Inverse scattering series methods are direct nonlinear inversion methods that do not require prior information of the potential. The major question when considering a series solution is the radius of convergence. Prosser (1969, 1976, 1980, 1982) showed that the convergence of the full inverse scattering series based on the Fredholm integral equation is very weak. The scattering interaction should be sufficiently small to allow the convergence of the Born–Neumann series of the acoustic Lippmann–Schwinger equation. To deal with this issue, Weglein and co-workers introduced the idea of subseries, which are associated with specific inversion tasks. The specific subseries, which are isolated from the whole inverse scattering series, converge.

Sams and Kouri (1969) showed that Lippmann–Schwinger equation can be transformed to a Volterra equation based on a renormalization technique. It has also been shown that the Born–Neumann series solution of the Volterra integral equation converges absolutely, irrespective of the magnitude of the coupling strength of the interaction. It is due to the property that the Volterra kernel is triangular. It has been proved in Kouri and Vijay (2003) that the 'Fredholm determinant' (Newton 1982) of the Volterra integral equation is equal to one, and the Born–Neumann expansion, which is identical with the Fredholm solution, possesses the most robust convergence properties. In that paper, the Volterra inverse scattering series was

derived for using both reflection and transmission data. However, only the first order of the VISS was examined for a simple square velocity model. In this paper, we undertake a further study and test of this approach, especially the effects of high order terms. The benefits of formulating acoustic scattering in terms of VISS appear substantial. The Green's function for the Volterra-based Lippmann–Schwinger equation is real and triangular. It allows efficient numerical implementation, which yields results in reasonable times. In addition, VISS is the method that deals with full data. The real data contains both primaries and multiples. Many inverse scattering methods process only the primaries (Shaw 2005, Amundsen *et al* 2005), which require the recorded data to undergo a pre-processing step to attenuate all multiples. However, we stress here that our method does not require the data to go through a multiple attenuating procedure. Finally, our method is a single comprehensive inversion method, and no task-oriented subseries needs to be separated.

Although the Born–Neumann series for a Volterra integral equation converges absolutely, the rate of convergence depends on the spatial part of the velocity potential and the square of the wavenumber. Also, although the choice of reference medium is arbitrary, it is better if it is close enough to the actual medium. However, it is still conventional to choose the reference velocity to be a homogeneous one, whose Green's function is known analytically. This often leads to a velocity potential, which describes the difference between the actual and reference medium that is too strong. Consequently, the Born–Neumann series will converge slowly. Besides, we also find that the assumption that the velocity potential can be expressed as a sum of orders of the data results in problems of convergence when the velocity potential increases. Instead of spending huge effort to evaluate high orders, convergence acceleration techniques can improve the rate of convergence of the inverse scattering series. These techniques can be used with advantage in certain cases to convert a slowly convergent series into a more rapidly converging one. Sometimes these techniques can also transform divergent series into convergent ones. In this paper, we study the impact of Cesàro summation (Evans 1970) and Euler transform methods (Kline 1983) on the convergence of our VISS (a brief introduction to these techniques is given in appendix A).

The paper is organized as follows: first, we give a brief review of the renormalization of the Lippmann–Schwinger equation for acoustic scattering. This is used as the mathematical framework to derive a Volterra Born–Neumann series for forward scattering. The VISS with both reflection and transmission data is derived based on the Born–Neumann series and the expansion of the velocity potential in orders of data assumption. We next analyze the result of the VISS for a single square velocity potential. Then we show numerically how the VISS method performs for several velocity models.

2. Volterra inverse scattering method

Consider a 1-D constant-density acoustic medium, where the velocity changes with depth, $c = c(z)$. The Helmholtz equation for the pressure wave $P(z, \omega)$ in the space-frequency domain is

$$\left[\frac{\partial^2}{\partial z^2} + \frac{\omega^2}{c^2(z)}\right] P = 0. \tag{1}$$

The spatially varying velocity $c(z)$ can be expressed in terms of a reference velocity c_0 and a velocity potential $V(z)$

$$\frac{1}{c^2(z)} = \frac{1}{c_0^2}\left[1 - V(z)\right]. \tag{2}$$

Then the Helmholtz equation can be rewritten as

$$\left[\frac{\partial^2}{\partial z^2} + k^2\right]P = k^2 V P, \tag{3}$$

where $k = \omega/c_0$ is the wavenumber. As is usual in the Lippmann–Schwinger scattering theory, the velocity potential is assumed to have compact support, which means the potential tends to zero sufficiently rapidly as $z \to \pm\infty$.

$$P_k^+(z) = P_0(k, z) + \int_{-\infty}^{\infty} \mathrm{d}z' G_{0k}^+(z, z') V(z') P_k^+(z'), \tag{4}$$

where $P_0(k, z) = \exp\left[\mathrm{i}kz\right]$ is the solution of the wave equation in the homogeneous medium:

$$\left[\frac{\partial^2}{\partial z^2} + k^2\right]P_0 = 0, \tag{5}$$

and G_{0k}^+ is the causal free Green's function multiplied by k^2

$$G_{0k}^+ = -\frac{\mathrm{i}k}{2}\mathrm{e}^{\mathrm{i}k|z-z'|}. \tag{6}$$

The pressure wave above the interaction can be represented as

$$P_k^+(z) = P_0(k, z) + R_k \mathrm{e}^{-\mathrm{i}kz}, \tag{7}$$

where R_k is the scattering reflection amplitude

$$R_k = -\frac{\mathrm{i}k}{2}\int_{-\infty}^{\infty} \mathrm{d}z \mathrm{e}^{\mathrm{i}kz} V(z) P_k^+(z), \tag{8}$$

When the receiver is located after the range of the interaction (z large enough that $V(z)$ tends to zero), we get the transmission amplitude

$$T_k = 1 - \frac{\mathrm{i}k}{2}\int_{-\infty}^{\infty} \mathrm{d}z \mathrm{e}^{-\mathrm{i}kz} V(z) P_k^+(z). \tag{9}$$

We eliminate the $|z - z'|$ argument in the causal Green's function in equation (6) to transform the Lippmann–Schwinger equation to a Volterra equation. This can be done by dividing the integration of equation (4) over z' into segments from $-\infty$ to z and from z to ∞

$$P_k^+(z) = \mathrm{e}^{\mathrm{i}kz} - \frac{\mathrm{i}k}{2}\int_{-\infty}^{z} \mathrm{d}z' \mathrm{e}^{\mathrm{i}k(z-z')} V(z') P_k^+(z') - \frac{\mathrm{i}k}{2}\int_{z}^{\infty} \mathrm{d}z' \mathrm{e}^{\mathrm{i}k(z'-z)} V(z') P_k^+(z'). \tag{10}$$

One then adds and subtracts $-(\mathrm{i}k/2)\int_z^{\infty} \mathrm{d}z' \mathrm{e}^{\mathrm{i}k(z-z')} V(z') P_k^+(z')$, and after simple manipulation, obtains

$$\begin{aligned} P_k^+(z) = \mathrm{e}^{\mathrm{i}kz} &- \frac{\mathrm{i}k}{2}\int_{-\infty}^{\infty} \mathrm{d}z' \mathrm{e}^{\mathrm{i}k(z-z')} V(z') P_k^+(z') \\ &- \frac{ik}{2}\int_{z}^{\infty} \mathrm{d}z' \left[\mathrm{e}^{\mathrm{i}k(z'-z)} - \mathrm{e}^{-\mathrm{i}k(z'-z)}\right] V(z') P_k^+(z'). \end{aligned} \tag{11}$$

Combining equations (9) and (11), we can obtain

$$\begin{aligned} P_k^+(z) &= T_k \mathrm{e}^{\mathrm{i}kz} + \int_{-\infty}^{\infty} \mathrm{d}z' \widetilde{G}_{0k}(z, z') V(z') P_k^+(z') \\ &= T_k \mathrm{e}^{\mathrm{i}kz} + k \int_z^{\infty} \mathrm{d}z' \sin\left[k(z' - z)\right] V(z') P_k^+(z'), \end{aligned} \tag{12}$$

where the new Green's function is given by

$$\widetilde{G}_{0k}(z, z') = k \sin\left[k(z' - z)\right] \eta(z' - z), \tag{13}$$

and $\eta(z)$ is the Heaviside function ($\eta(z) = 0$ for $z < 0$, $\eta(z) = 1$ for $z \geqslant 0$).

Equation (12) is an inhomogeneous Volterra integral equation of the second kind, and it is identical to the original Lippmann–Schwinger equation (one physical explanation of the renormalization is given in appendix B). Since T_k is constant for a given frequency, we can try a solution of the following form to solve equation (12):

$$P_k^+(z) = \widetilde{P}_k(z) T_k. \tag{14}$$

Substituting equation (14) into the renormalized Lippmann–Schwinger equation (12), we obtain

$$\widetilde{P}_k(z) = P_0 + \int_{-\infty}^{\infty} \mathrm{d}z' \widetilde{G}_{0k}(z, z') V(z') \widetilde{P}_k(z') \tag{15}$$

Iterating equation (15), we can get the Born–Neumann series for $\widetilde{P}_k$ (Taylor 2012)

$$\begin{aligned} \widetilde{P}_k &= P_0 + \widetilde{G}_{0k} V P_0 + \widetilde{G}_{0k} V \widetilde{G}_{0k} V P_0 + \cdots \\ &= \sum_{n=0}^{\infty} \left(\widetilde{G}_{0k} V\right)^n P_0. \end{aligned} \tag{16}$$

In the above equation, we employ an abstract notation, where the coordinates and integral operator are suppressed.

Because of the triangular nature of $\widetilde{G}_{0k}$, the Born–Neumann series of equation (12) converges absolutely and uniformly on any compact set of z and for non-compactly supported V, provided V decays faster than $|z|^{-2}$ for large $|z|$ (Newton 1982, Kouri and Vijay 2003).

2.1. The Volterra inverse scattering series for reflection and transmission data

Substituting equation (16) into equation (8), we obtain

$$\frac{2i}{k} \frac{R_k}{T_k} = \int_{-\infty}^{\infty} \mathrm{d}z' \mathrm{e}^{\mathrm{i}kz'} V(z') \sum_{n=0}^{\infty} \left(\widetilde{G}_{0k} V\right)^n P_0. \tag{17}$$

To solve the above equation, we replace $\frac{2\mathrm{i}}{k}\frac{R_k}{T_k}$ in equation (17) by $\epsilon \frac{2\mathrm{i}}{k}\frac{R_k}{T_k}$, where ϵ is an 'ordering parameter', which ultimately is set equal to one. Furthermore, we also assume that we can express V as a power series in orders of the data (The convergence of this power series of V is different from the convergence of the Born–Neumann series of P_k, and is not considered in detail here):

$$V = \sum_{j=1}^{\infty} \epsilon^j V_j. \tag{18}$$

Plugging the above equation into equation (17), we obtain:

$$\epsilon\frac{2\mathrm{i}}{k}\frac{R_k}{T_k} = \int_{-\infty}^{\infty}\mathrm{d}z'\mathrm{e}^{\mathrm{i}kz'}\sum_{j=1}^{\infty}\epsilon^j V_j\sum_{n=0}^{\infty}\left(\widetilde{G}_{0k}\sum_{j'=1}^{\infty}\epsilon^{j'}V_{j'}\right)^n P_0. \tag{19}$$

Collecting coefficients of each power of ϵ yields:

$$\varepsilon^1\colon\ V_1(2k) = \frac{2\mathrm{i}}{k}\frac{R_k}{T_k}, \tag{20}$$

$$\varepsilon^2\colon\ V_2(2k) = -\int\mathrm{d}z'\int\mathrm{d}z''\mathrm{e}^{\mathrm{i}k(z'+z'')}V_1(z')\,\widetilde{G}_{0k}\,V_1(z''), \tag{21}$$

$$\begin{aligned}\varepsilon^3\colon\ V_3(2k) = &-\int\mathrm{d}z'\int\mathrm{d}z''\mathrm{e}^{\mathrm{i}k(z'+z'')}V_2(z')\,\widetilde{G}_{0k}\,V_1(z'')\\ &-\int\mathrm{d}z'\int\mathrm{d}z''\mathrm{e}^{\mathrm{i}k(z'+z'')}V_1(z')\,\widetilde{G}_{0k}\,V_2(z'')\\ &-\int\mathrm{d}z'\int\mathrm{d}z''\int\mathrm{d}z'''\mathrm{e}^{\mathrm{i}k(z'+z''')}V_1(z')\,\widetilde{G}_{0k}\,V_1(z'')\,\widetilde{G}_{0k}\,V_1(z'''),\end{aligned} \tag{22}$$

etc.

Note that the Green's function of the VISS with R_k/T_k differs from the causal free Green's function of ISS. These matrix element expressions for each order are first evaluated in the k domain

$$V_j(2k) = \int_{-\infty}^{\infty}\mathrm{d}z\mathrm{e}^{2\mathrm{i}kz}V_j(z), \qquad j = 1,\ 2,\ 3,\ \cdots. \tag{23}$$

The result can be transformed to the spatial domain by the inverse Fourier transform

$$V_j(z) = \frac{1}{\pi}\int_{-\infty}^{\infty}\mathrm{d}k\mathrm{e}^{-2\mathrm{i}kz}V_j(2k), \qquad j = 1,\ 2,\ 3,\ \cdots \tag{24}$$

3. Analysis of analytical results for the Volterra inverse scattering series

In this section, we present the results of the VISS method for a single square barrier or well. The expression for the single square barrier or well velocity potential is $V(z) = V_0\eta(z)\,\eta(a - z)$, where V_0 is the velocity interaction amplitude, and a is its width, and $\eta(z)$ is the Heaviside function. The reflection and transmission coefficients can be computed analytically (Ferry 1995, McMurry 1994)

$$R_k = \frac{V_0\sin\left(ak\sqrt{1-V_0}\right)}{(2-V_0)\sin\left(ak\sqrt{1-V_0}\right) + 2\mathrm{i}\sqrt{1-V_0}\cos\left(ak\sqrt{1-V_0}\right)}, \tag{25}$$

$$T_k = \frac{2\sqrt{1-V_0}\mathrm{e}^{-\mathrm{i}ka}}{V_0\sin\left(ak\sqrt{1-V_0}\right)}R_k. \tag{26}$$

Using the Volterra inverse scattering series with R_k/T_k (equation (20) to equation (22)), we obtain the VISS results for the first three orders for the square well or barrier

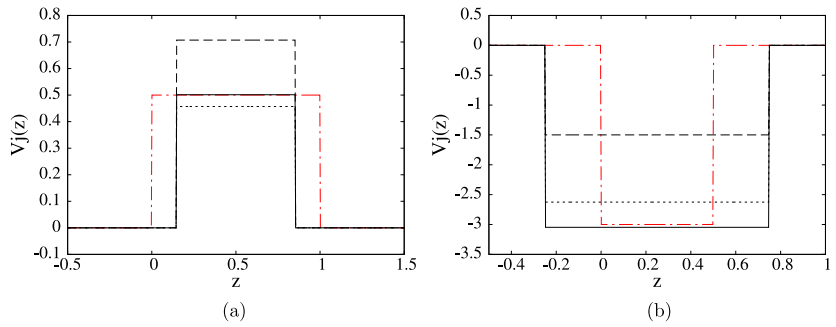

Figure 1. Comparison of the exact barrier (dash-dot line) with the first order (dashed line), the sum of first two orders (dotted line), the sum of first three orders (solid line) obtained through the VISS for square barrier test cases: (a) $V_0 = 0.5$, $a = 1.0$, (b) $V_0 = -3$, $a = 0.5$.

$$V_1(z) = \frac{V_0}{\sqrt{1 - V_0}}\eta(z - z_1)\,\eta(z_2 - z), \tag{27a}$$

$$\begin{aligned} V_2(z) = &-\frac{V_0^2}{2(1 - V_0)}\eta(z - z_1)\,\eta(z_2 - z) \\ &+\frac{V_0^2}{4(1 - V_0)}(z_2 - z_1)\left[\delta(z_1 - z) + \delta(z_2 - z)\right], \end{aligned} \tag{27b}$$

$$\begin{aligned} V_3(z) = &\frac{1}{8}\left(\frac{V_0}{\sqrt{1 - V_0}}\right)^3\eta(z - z_1)\,\eta(z_2 - z) \\ &-\frac{1}{16}\left(\frac{V_0}{\sqrt{1 - V_0}}\right)^3(z_2 - z_1)\left[\delta(z_1 - z) + \delta(z_2 - z)\right] \\ &+\frac{1}{32}\left(\frac{V_0}{\sqrt{1 - V_0}}\right)^3(z_2 - z_1)^2\left[\delta'(z_2 - z) - \delta'(z_1 - z)\right], \end{aligned} \tag{27c}$$

where $\eta(z)$ is the Heaviside function and $z_1 = \frac{a}{2}\left(1 - \sqrt{1 - V_0}\right)$, $z_2 = \frac{a}{2}\left(1 + \sqrt{1 - V_0}\right)$. For a barrier, $0 < V_0 < 1$ so that the first-order result has a higher barrier than the true one. For a well, $V_0 < 0$ and the first order result is shallower than the true well. Thus, although the first-order result has the correct analytical form of a square well or barrier, it has an incorrect width and height (or depth). The second order result contains two contributions: (1) the Heaviside terms (similar to the first order), (2) the Dirac-δ function and its derivatives. As explained in Weglein *et al* (2000), the Heaviside terms are corrections to the amplitude of the velocity potential, and the Dirac-δ terms can be treated as terms in a Taylor expansion of the Heaviside function. Thus, the Dirac-δ terms perform the task of correctly locating the reflectors (i.e. the beginning and ending of the barrier or well). Higher order terms in the VISS will contribute additional Heaviside and Dirac-δ functions and their derivatives which improve the quality of the imaging.

For different values of V_0, we compare the plots of the exact barrier or well, and the Heaviside terms of the first three orders $V_j(z)$ obtained through the VISS with R_k/ T_k data

Table 1. Amplitude error in function of the number of V_j terms correction. Here, the error percentage $E_i = |(\sum_{j=1}^{i} V_j - V_0)/V_0|$.

V_0	$A(V_1)$	$A(V_2)$	$A(V_3)$	E_1 (%)	E_2 (%)	E_3 (%)
0.5	0.707	−0.25	0.044	41.4	8.6	0.2
−3.0	−1.500	−1.125	−0.422	50	12.5	1.57

(figure 1). We observe that for a lower velocity potential case ($V_0 = 0.5$), the VISS shows excellent convergence after summing the first three orders. Note that for $V_0 = 0.5$, one has $c_1 = \sqrt{2}\, c_0$ and for $V_0 = -3$, one has $c_1 = c_0/2$. Table 1 shows the amplitude error as a function of the number of V_j terms included. Although the differences between the actual velocity and the sum of first three orders increases for higher velocity contrast (case $V_0 = -3$), the percent error is actually rather small. Furthermore, we can continue computing more terms if we want to reach higher accuracy.

The errors in the depth (onset of the barrier or well and end of the barrier or well) are symmetrical when the initial and final values of the velocity are equal and one uses R_k/T_k data. In the case of a barrier, the height of the first term $|A(V_1)| > V_0$ and thus $c(z)$ are over-estimated. The barrier width is smaller than the exact one, since the corrected term is for a P-wave traveling faster than it should. In the case of a well, the height of the first term $|A(V_1)| < |V_0|$ and thus $c(z)$ is under-estimated. It results in the predicted well width to be wider. As mentioned above, the Dirac-δ function and its higher derivatives are associated with a Taylor expansion of Heaviside functions which correct the error in the depth. This can be demonstrated by using the expansion of the Heaviside function as a Taylor series. The Taylor series for a Heaviside function $f(z) = \eta(z - z_0)$ expanded about $\hat{z}_0$ can be written as:

$$f(z) = \eta(z - z_0) = \sum_{n=0}^{\infty} \frac{(z_0 - \hat{z}_0)^n}{n!} \frac{\partial^n f(z)}{\partial z^n}\bigg|_{z=\hat{z}_0}$$

$$= \eta(z - \hat{z}_0) + \delta(z - \hat{z}_0)(z_0 - \hat{z}_0) + \delta'(z - \hat{z}_0)\frac{(z_0 - \hat{z}_0)^2}{2} + O\left[(z_0 - \hat{z}_0)^3\right]. \quad (28)$$

On the left hand side of the inverse series results, we write the correction between the incorrectly-placed Heaviside and the correct Heaviside function as:

$$C_{left}(z) = V_0\left[\eta(z_1 - z) - \eta(z_0 - z)\right) = -V_0\left[\eta(z_0 - z) - \eta(z_1 - z)\right], \quad (29)$$

with $z_0 = 0$ the exact depth. Its Taylor series around z_1 is given by:

$$C_{left}(z) = -V_0\left[\delta(z - z_1)(z_1 - z_0) + \delta'(z - z_1)\frac{(z_1 - z_0)^2}{2} + O\left((z_0 - \hat{z}_0)^3\right)\right]. \quad (30)$$

From

$$z_1 = \frac{a}{2}\left(1 - \sqrt{1 - V_0}\right), \qquad z_2 = \frac{a}{2}\left(1 + \sqrt{1 - V_0}\right), \quad (31)$$

Table 2. Comparison of the values of $\delta(z - z_1)$ and $\delta'(z - z_1)$ coefficients for each case.

	V_0	a	Exact	V_2	Error (%)	$V_2 + V_3$	Error (%)
$\delta(z - z_1)$	0.5	1	0.0732	0.0884	20.77	0.0728	0.55
	−3	0.5	0.75	0.5625	25	0.7473	3.12
$\delta'(z - z_1)$	0.5	1	−0.0054	—	—	−0.0055	1.85
	−3	0.5	0.0938	—	—	0.1055	12.47

we obtain

$$z_1 - z_0 = \frac{1 - \sqrt{1 - V_0}}{2\sqrt{1 - V_0}}(z_2 - z_1). \tag{32}$$

Then we find an expression for the exact coefficients of the Taylor series correction in $\delta^n(z - z_1)$ truncated at the second order:

$$C_{left}(z) = -V_0\left[\delta(z - z_1)\frac{z_2 - z_1}{2}\left(\frac{1 - \sqrt{1 - V_0}}{\sqrt{1 - V_0}}\right) + \delta'(z - z_1)\frac{(z_2 - z_1)^2}{8}\left(\frac{1 - \sqrt{1 - V_0}}{\sqrt{1 - V_0}}\right)^2 + O\left((z_2 - z_1)^3\right)\right]. \tag{33}$$

In table 2, we list the $\delta(z - z_1)$ and $\delta'(z - z_1)$ coefficients from first three orders and its percentage error with respect to the exact values for these two velocity examples,.

From the analysis above, we find that the Dirac-δ function and its derivative terms perform the task of depth correction. For low velocity contrast, the differences of the coefficients between the exact Dirac-δ function and its derivative terms and the series result are rather small, which means that we can obtain a reasonably accurate depth with only few orders. The values of δ and δ' coefficients for the correction of the right side will be the same since the width error is symmetrical. Combining these analyses for a single square velocity potential, we find that the Volterra inverse scattering series with R_k/T_k converges nicely to the exact interaction. For low velocity contrast, the Volterra inverse series shows excellent convergence with only a few terms. For high velocity contrast, we need higher order terms to obtain the desired accuracy.

Numerical results for the Volterra inverse scattering series

In this section, we illustrate the performance of the present VISS method numerically by applying it to two different types of velocity models: smooth interactions (Gaussian), and a smooth, but more rapidly varying, interaction (smoothed barrier). The synthetic reflection and transmission data of these velocity models are generated based on the Volterra forward scattering algorithm introduced in Yao *et al* (2013).

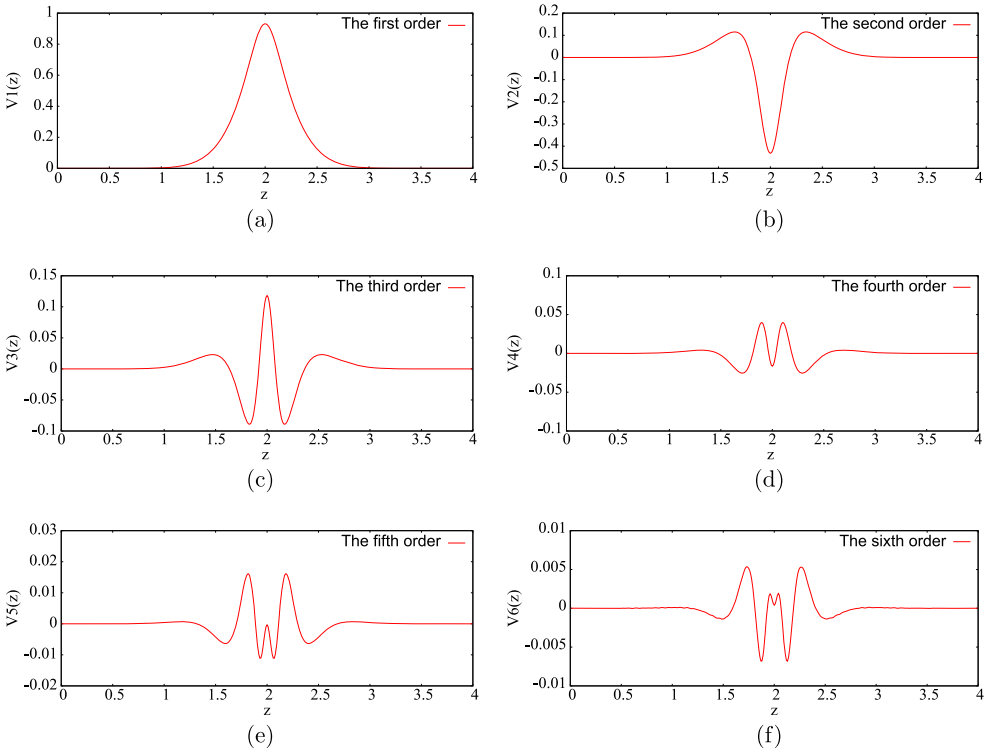

Figure 2. The first six orders of VISS with R_k/T_k for the Gaussian interaction with $V_0 = 0.6$, $a = 2$, $b = 1/2$: (a) first order; (b) second order; (c) third order; (d) fourth order; (e) fifth order; (f) sixth order.

3.1. Application of the VISS to the Gaussian velocity interaction

We report results of our VISS for several different amplitudes V_0 of the following Gaussian velocity interaction

$$V(z) = V_0 \mathrm{e}^{-\frac{(z-a)^2}{b^2}}. \tag{34}$$

Figure 2 shows the numerical VISS results of the first six orders for the Gaussian velocity potential with an amplitude parameter $V_0 = 0.6$. The exact interaction and cumulative sums of the first six orders are displayed in figure 3. For this model, VISS converges rapidly to the true velocity potential. The mis-estimation of the velocity has been corrected after summing six terms. More terms in the VISS for this model are not necessary. Table 3 shows the corresponding L^2-distance[5] for $V_0 = 0.6$ of the cumulative sums of the first six orders and the Cesàro summation starting from the first partial sum relative to the exact Gaussian velocity contrast. We find that the summation techniques are not required, and in fact they do not improve the convergence for this rapidly convergent case.

Figure 4 shows the results of the VISS for the Gaussian velocity potential with an amplitude parameter $V_0 = -2$, and the corresponding L^2-distance is given in table 4. figure 4(a) is the comparison of the exact velocity potential and the first order of VISS. For

[5] The L^2-distance between two function $f(x)$ and $g(x)$ is $\| f - g \|_2 = \sqrt{\int_a^b |f(x) - g(x)|^2 dx}$

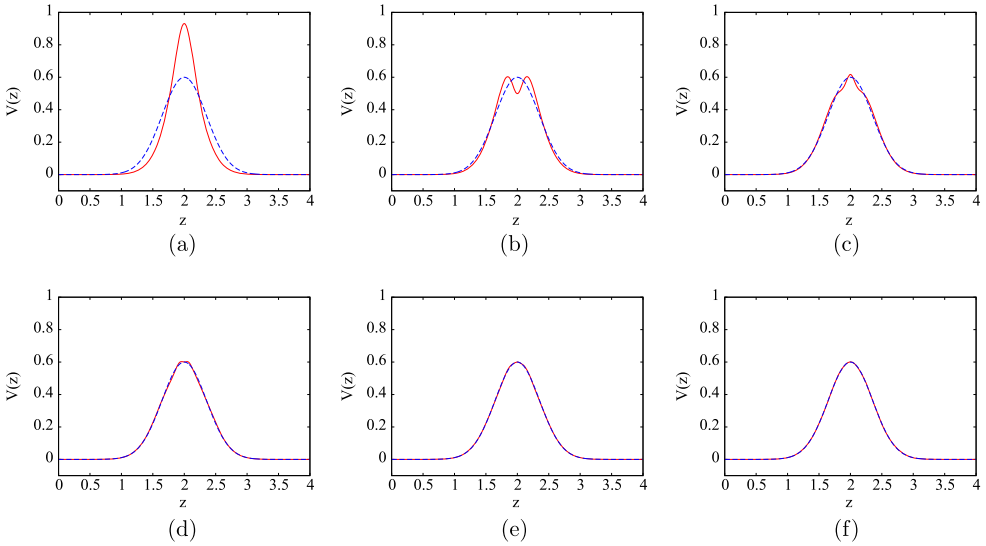

Figure 3. The exact Gaussian interaction (dashed) with $V_0 = 0.6$, $a = 2$, $b = 1/2$ compared with: (a) first order; (b) sum of first two orders; (c) sum of first three orders; (d) sum of first four orders; (e) sum of first five orders; (f) sum of first six orders.

Table 3. The L^2-distance in terms of V_j terms correction for the Gaussian interaction of $V_0 = 0.3$.

Orders included	V_1	$\sum_{j=1}^{2} V_j$	$\sum_{j=1}^{3} V_j$	$\sum_{j=1}^{4} V_j$	$\sum_{j=1}^{5} V_j$	$\sum_{j=1}^{6} V_j$
VISS	0.167 22	0.053 55	0.019 5	0.008 07	0.003 38	0.001 34
Cesàro	0.167 22	0.081 12	0.050 88	0.037 90	0.030 47	0.025 46

this large amplitude velocity potential case, the difference between the exact and the first order approximation is relatively large. And we observe that the VISS gives a good correction of the Gaussian amplitude after summing six orders (figure 4(b)). However, the higher orders have large oscillations which make it difficult to get a satisfactory result on either side of the maximum of the exact velocity potential after just summing the first few orders of the original series. figure 4(c) shows the sixth order Cesàro's summation of the VISS. For this high velocity contrast, the Cesàro summation gives a better solution by reducing the oscillation. On the other hand, the Cesàro summation causes error in the amplitude. figure 4(d) shows the Cesàro's summation with a different starting partial sum. We observe that for this case, the Cesàro's summation starting with high order partial sums gives a better result. figure 4(e) gives the result of the Euler transform of the VISS up to six orders. Compared with Cesàro's summation, the Euler transform does not provide any advantage in improving the rate of convergence for this Gaussian well case. The study of these two velocity potential models highlights the need for a method to improve convergence at high contrast. The Cesàro summation and Euler transform methods are helpful for this smooth interaction case.

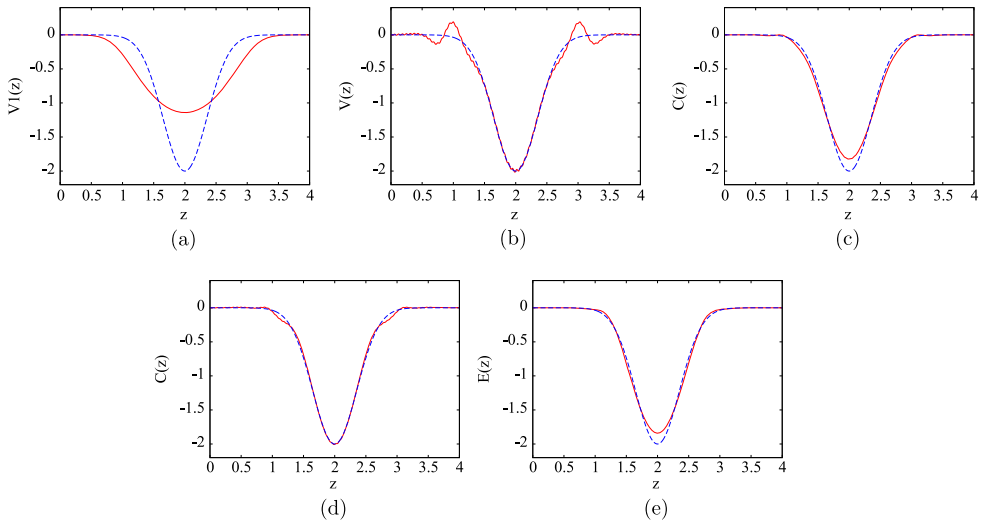

Figure 4. The exact Gaussian interaction with amplitude $V_0 = -2$ (dashed line) compared with (a) first order; (b) the sum of the first six orders; (c) C_6^1 Cesàro summation; (d) C_6^4 Cesàro summation; (e) the Euler transform up to six orders.

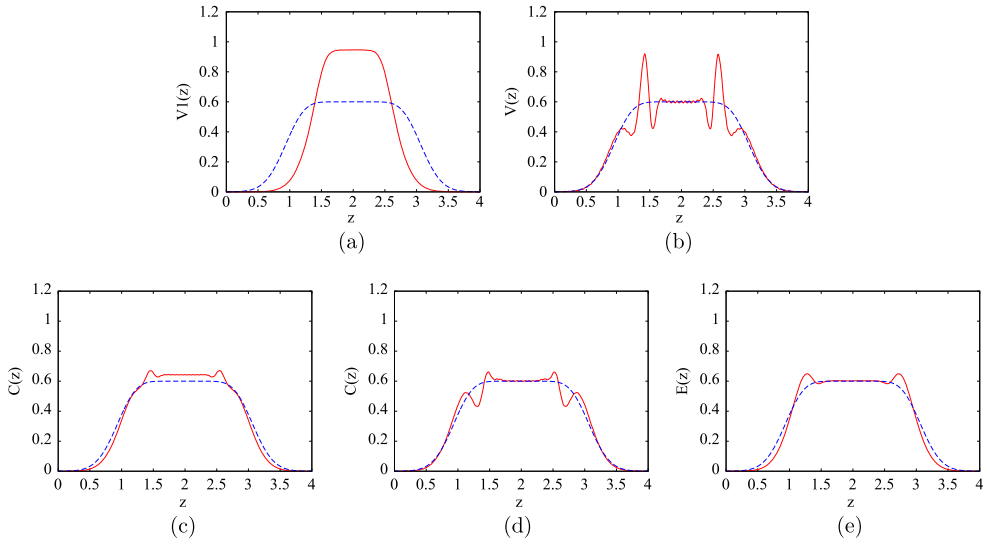

Figure 5. Comparison of the exact model 1 (dashed line) and the result of VISS with R_k/T_k data: (a) first order of VISS; (b) sum of the first six orders; (c) C_6^1 Cesàro summation; (d) C_6^4 Cesàro summation; (e) the Euler transform.

Table 4. The L^2-distance of the results for the Gaussian interaction of $V_0 = -2$.

Model	V_1	$\sum_{j=1}^{6} V_j$	C_6^1	C_6^4	Euler
Gaussian $V_0 = -2$	0.653 77	0.148 17	0.117 36	0.053 98	0.099 59

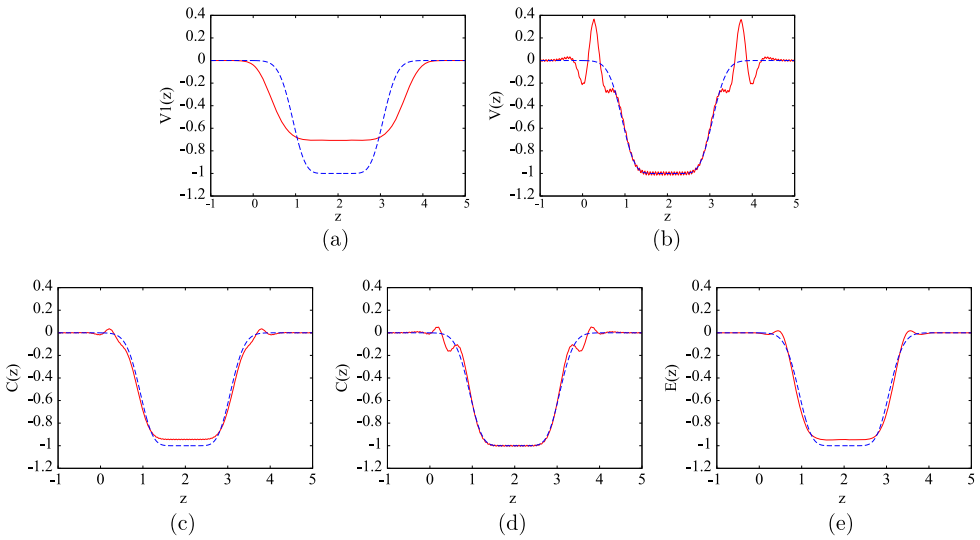

Figure 6. Comparison of the exact model 2 (dashed line) and the result of VISS with R_k/T_k data: (a) first order of VISS; (b) sum of the first six orders; (c) C_6^1 Cesàro summation; (d) C_6^4 Cesàro summation; (e) the Euler transform.

3.2. Application of VISS to the smoothed barrier interaction

To further test our method's sensitivity to sharper changes in the velocity potential, we evaluate it with two smoothed barrier interaction models. figure 5 shows the comparison for the exact interaction model 1 to the first order of VISS, to the sum of the first six orders of VISS, and to the C_6^1 and C_6^4 Cesàro summations and Euler transform of VISS up to six order. table 5 gives the corresponding L^2-distance. Similar to the Gaussian velocity potential, the result of just summing the original series suffers from large oscillations. The Cesàro summation starting from the first partial sum gives a smoother result but has a small error compared to the exact amplitude of the interaction. The Cesàro summation starting from the fourth partial sums offers a reasonable balance between smoothing and amplitude correction for this case. For this case the Euler transform of VISS gives a relatively better solution for both amplitude and oscillations.

Figure 6 compares results of the interaction model 2 with a maximum contrast of −1, to the first order of the VISS, to the sum of first six orders of VISS, and to the C_6^1, to the C_6^4 Cesàro summations and to the Euler transform up to six orders. Here the first order amplitude is in less good agreement with the exact value of −1. Large oscillations appear in the direct summing of the VISS. Similar to other cases, we observe that the Cesàro summation method and Euler transform improve this case (see table 5).

4. Discussion

We tested our Volterra inverse scattering series for reflection and transmission data on several 1D velocity potentials. We want to stress that the data we use here is the so-called 'full data'. We do not need to go through a pre-processing step to remove internal multiples of the recorded data. Also, the inversion method we presented is a single comprehensive task. In

Table 5. The L^2-distance results for smoothed barrier interaction.

Model	V_1	$\sum_{j=1}^{6} V_j$	C_6^1	C_6^4	Euler
Model 1	0.435 99	0.167 42	0.071 09	0.082 76	0.077 17
Model 2	0.514 02	0.249 14	0.096 39	0.010 123	0.098 68

other words, no task-oriented subseries were separated. Furthermore, we do not assume that the actual medium differs from the reference medium only at locations of rapid change. Indeed, our method provides good performance for a smooth-varying velocity potential. The VISS proved to improve the convergence of inverse acoustic scattering problem thanks to the absolute convergence property of its Volterra kernel. The series acceleration technique is not necessary for low velocity contrasts where the original VISS already converges very rapidly. However, we do not get satisfactory results with just a few orders when the interaction is relatively strong and presents sharp variations. These are the consequences of the slower rate of convergence of Born–Neumann series and the poorer convergence of the 'order of data' assumption for the velocity potential. It is useful to employ series acceleration techniques for improving the convergence of the VISS for slowly convergent cases. The Cesàro summation method improvement of the VISS result is straightforward, especially starting with high order partial sums. The Euler transform method can give a better result for barrier velocity potential cases, where the original series is an alternating series. Besides, these techniques are also useful to reduce the Gibbs oscillations due to the truncating of the range of integration over wavenumber. In Lesage *et al* (2013) and Yao *et al* (2013), we also derived the VISS with only the reflection data. We found that the VISS with both reflection and transmission data shows better convergence than just using reflection data only. Hence, if possible, recording both reflection and transmission data simultaneously can increase the quality of inversion.

5. Conclusion and future work

This paper contains a brief review of the Volterra inverse scattering series using both reflection and transmission data for a one dimensional acoustic medium. As stated by Weglein (2013), the inverse scattering series is a direct nonlinear inversion method, and it requires no prior information of the target. Results for a few velocity models showed that the potential can be estimated by using the Volterra inverse scattering series (VISS). Although the models used in the numerical tests are simple, the results are encouraging. For low-velocity contrast, the direct summation of VISS gives a velocity estimation with high precision. The series acceleration techniques, (e.g, Cesàro summation and Euler transform) show the ability to improve the rate of convergence for high-velocity contrast. Besides, they also demonstrated their capability in reducing Gibbs oscillations. In the present study, we have restricted our attention to 1D acoustic scattering. In the future, we will extend our method to higher dimensions as well as to elastic wave scattering cases.

Acknowledgments

We thank Total and PGS for their support and the authorization to publish this work. Partial support of this research under R A Welch Foundation Grant E-0608 is gratefully acknowledged. The author D J K is indebted to and thanks A B Weglein for introducing him to inverse scattering based on the Born–Neumann expansion.

Appendix A. Brief review of series summation techniques

In this appendix, we give a few more details regarding the series acceleration techniques we employed in the paper. One method is the Cesàro method of summation. The *N*th partial sum of the VISS can be represented as

$$\begin{aligned} S_n(z) &= \sum_{j=1}^{n} V_j(z) \\ &= \frac{1}{\pi}\sum_{j=1}^{n}\int_{-\infty}^{\infty} \mathrm{d}k V_j(2k)\, e^{-2ikz}. \end{aligned} \tag{A.1}$$

The series of equation (A.1) has a problem of convergence when the velocity potential is relatively strong. This difficulty may be partially resolved by using the Cesàro summation method which defines the derived series as the limit of the sequence of arithmetic means of the sequences of partial sums of the series. That is

$$C(z) = \lim_{N\to\infty} C_N(z) = \lim_{N\to\infty} \frac{1}{N}\sum_{n=1}^{N} S_n(z). \tag{A.2}$$

The sequence of arithmetic means converges to the same value as the sequence of partial sums if the latter converges and may still converge even if the series diverges. The Nth Cesàro sum of the VISS may be written as

$$C_N(z) = \frac{1}{\pi}\int_{-\infty}^{\infty} \mathrm{d}k D_N e^{-2ikz}, \tag{A.3}$$

where the kernel D_N is given by

$$D_N(k, z) = \frac{1}{N}\sum_{j=1}^{N}(N + 1 - j)\, V_j(2k). \tag{A.4}$$

If the series is Cesàro sumable, it can be easily verified that the arithmetic mean of the partial sums of the series with different starting terms will converge to the same value

$$C(z) = \lim_{N\to\infty} C_N^{\alpha}(z) = \lim_{N\to\infty} \frac{1}{N + 1 - \alpha}\sum_{n=\alpha}^{N} S_n(z);\ \alpha = 1, 2, 3, \ldots \tag{A.5}$$

Another technique is the Euler transform. The Euler transform of the Volterra inverse scattering series $\sum_{j=1}^{\infty} V_j$ can be represented as

$$\sum_{j=1}^{\infty} V_j = \sum_{j=1}^{\infty} \frac{\Delta^j V_1}{2^j}, \tag{A.6}$$

where

$$\Delta^1 V_1 = V_1,\ \Delta^2 V_1 = V_2 + V_1,\ \Delta^n V_1 = \sum_{j=0}^{n}\binom{n}{j} V_{j+1},\ n \geqslant 2. \tag{A.7}$$

These two summation methods can be used with advantage for the Volterra inverse scattering series due to sequences of alternating higher order terms as well as in non-convergent cases. They can also decrease the Gibbs phenomenon that arises for example in the case of sharp velocity changes.

Appendix B. The physical meaning of renormalization of Lippmann–Schwinger equation

Here, we provide a physical explanation for the renormalization of the Lippmann–Schwinger equation. The Volterra Green's function (13) can be considered as a combination of the free causal and anti-causal Green's function

$$\widetilde{G}_{0k}(z, z') = \left(G_{0k}^{+} + G_{0k}^{-}\right)\eta(z' - z), \tag{B.1}$$

where G_{0k}^{-} is the free anti-causal Green's function multiplied by k^2.

Plugging equation (B.1) into the renormalized Lippmann–Schwinger equation (12), we obtain

$$P_k^{+}(z) = T_k e^{ikz} + \int_z^{\infty} dz' \left(G_{0k}^{+} + G_{0k}^{-}\right) V P_k^{+}, \tag{B.2}$$

Comparing with the original Lippmann–Schwinger equation (4), it means that the incident wave propagating in the interaction above z is identical with the transmitted wave migrated to depth z. In a particular case, considering the pressure wave at depth z_0, which is above the interaction, the original Lippmann–Schwinger equation is

$$P_k^{+}(z_0) = P_0 + \int_{z_0}^{\infty} dz' G_{0k}^{+} V P_k^{+}, \tag{B.3}$$

and the renormalized Lippmann–Schwinger equation is

$$P_k^{+}(z_0) = T_k e^{ikz_0} + \int_{z_0}^{\infty} dz' G_{0k}^{-} V P_k^{+} + \int_{z_0}^{\infty} dz' G_{0k}^{+} V P_k^{+}. \tag{B.4}$$

Then we have

$$P_0 = T_k e^{ikz_0} + \int_{z_0}^{\infty} dz' G_{0k}^{-} V P_k^{+}. \tag{B.5}$$

It means that the incident pressure wave P_0 can be represented by the transmitted pressure wave $T_k e^{ikz_0}$ migrated with the anti-causal Green's function G_{0k}^{-}.

References

Amundsen L, Reitan A, Helgesen H K and Arntsen B 2005 *Inverse Problems* **21** 1823–50

Bleistein N 1984 *Mathematical Methods for Wave Phenomena* (*Computer Science and Applied Mathematics*) (Orlando, FL: Academic)

Clayton R and Stolt R 1981 *Geophysics* **46** 1559–67

Cohen J K and Bleistein N 1977 *SIAM J. Appl. Math.* **32** 784–99

Colton D and Kress R 1998 *Inverse Acoustic and Electromagnetic Scattering Theory (Applied Mathematical Sciences)* (New York: Springer)

Colton D and Monk P 1989 *Inverse Problems* **5** 1013

Evans C M 1970 *J. Franklin Inst.* **289** 185–191

Ferry D 1995 *Quantum Mechanics: An Introduction for Device Physicists and Electrical Engineers* (New York: Taylor and Francis)

Guitton A and Alkhalifah T 2013 *Leading Edge* **32** 1026–8

Jost R and Kohn W 1952 *Phys. Rev.* **87** 977–92

Kline M 1983 *Math. Mag.* **56** 307–14

Kouri D J and Vijay A 2003 *Phys. Rev.* E **67** 046614

Lesage A, Yao J, Eftekhar R, Hussain F and Kouri D 2013 *SEG Expanded Abstracts* **899** 4645–9

McMurry S 1994 *Quantum Mechanics* (Boston, MA: Addison-Wesley)

Moses H E 1956 *Phys. Rev.* **102** 559–67

Newton R G 1982 *Scattering Theory of Waves and Particles* (New York: Springer)
Pratt R G 1999 *Geophysics* **66** 888–901
Prosser R T 1969 *J. Math. Phys.* **10** 1819–22
Prosser R T 1976 *J. Math. Phys.* **17** 1775–9
Prosser R T 1980 *J. Math. Phys.* **21** 2648–53
Prosser R T 1982 *J. Math. Phys.* **23** 2127–30
Razavy M 1975 *J. Acoust. Soc. Am.* **58** 956
Sams W N and Kouri D J 1969 *J. Chem. Phys.* **51** 4809–14
Shaw S A 2005 An inverse scattering series algorithm for depth imaging of reflection data from a layered acoustic medium with an unknown velocity model *PhD thesis* University of Houston
Sirgue L and Pratt R G 2004 *Geophysics* **69** 231–48
Tarantola A 1984 *Geophysics* **49** 1259–66
Taylor J 2012 *Scattering Theory: The Quantum Theory of Nonrelativistic Collisions* (New York: Dover)
Virieux J and Operto S 2009 *Geophysics* **74** WCC1–26
Weglein A 2013 *Leading Edge* **32** 1192–204
Weglein A B, Foster D, Matson K, Shaw S, Carvalho P and Corrigan D 2001 *SEG Expanded Abstracts* **541** 2108–11
Weglein A B, Matson K H and Matson D J 2000 *SEG Expanded Abstracts* **260** 1016–9
Weglein A B 2003 *Inverse Problems* **19** R27
Weglein A, Gasparotto F, Carvalho P and Stolt R 1997 *Geophysics* **62** 1975–89
Yao J, Lesage A C, Bodmann B G, Hussain F and Kouri D J 2014 Direct nonlinear inversion of acoustic media using volterra inverse scattering series. I. One dimensional data *Geophysics* submitted
Zhang H and Weglein A 2009 *Geophysics* **74** WCD29–39